A

	OsPHO2			
HvPHO2	79.06%/85.35%	**HvPHO2**		
ZmPHO2	77.00%/85.81%	77.80%/83.75%	**ZmPHO2**	
AtPHO2	45.10%/62.16%	44.15%/61.53%	44.72%/62.57%	**AtPHO2**
NbPHO2	45.42%/62.20%	44.77%/61.66%	45.68%/62.08%	49.22%/66.08%

B

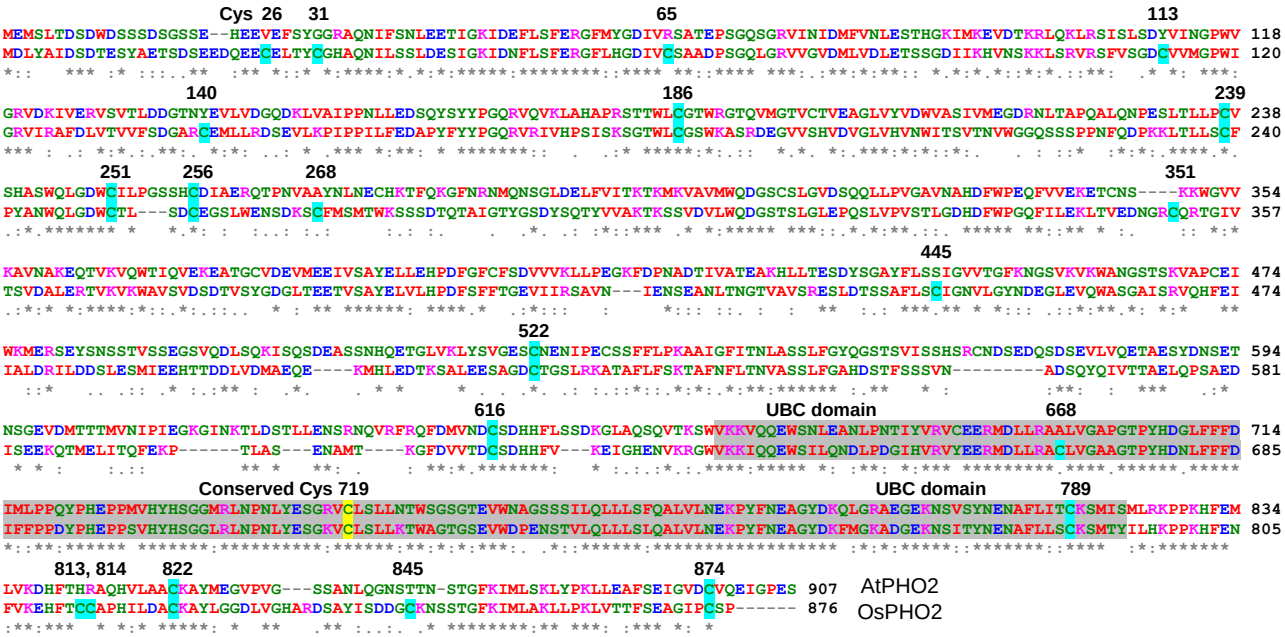

C

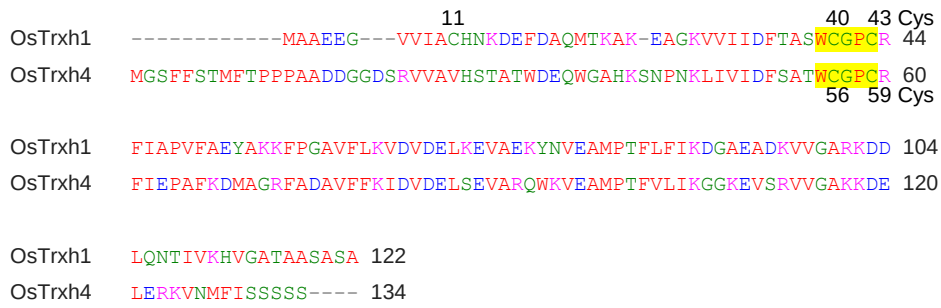

Supplemental Figure S1. Alignments of amino acid sequences.
A, The identity/similarity matrix for plant PHO2 proteins from *Oryza sativa* (Os), *Hordeum vulgare* (Hv), *Zea mays* (Zm), *Arabidopsis thaliana* (At), and *Nicotiana benthamiana* (Nb).
B, Amino acids sequences alignment of PHO2 proteins in Arabidopsis and rice. UBC domains and cysteine residues are highlighted.
C, Amino acid sequences alignment between OsTrxh1 and OsTrxh4. Cysteine residues in the conserved active domain "WCGPC" are indicated.

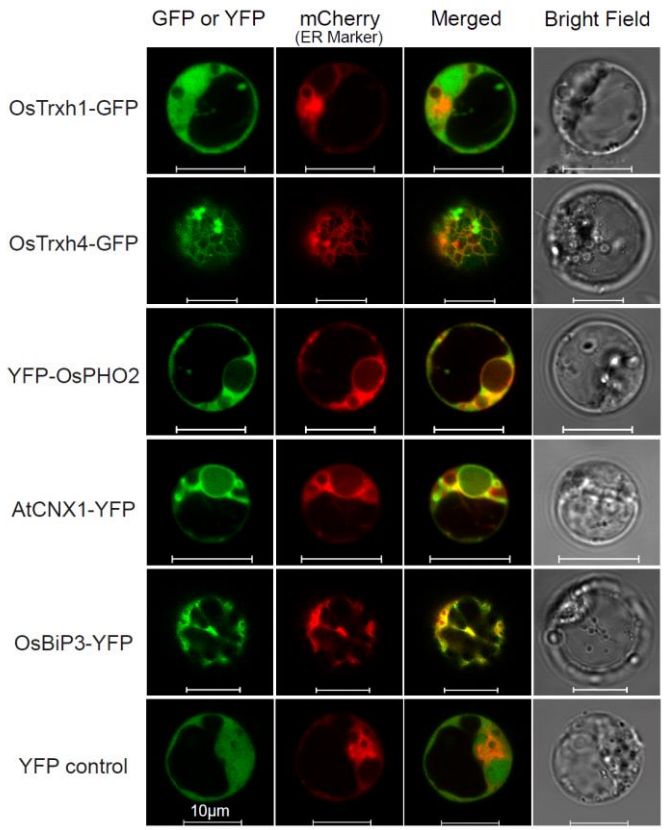

Supplemental Figure S2. Subcellular localization of OsPHO2, OsTrxh1 and OsTrxh4-FP fusion proteins in rice protoplasts. The plasmid pSAT6-EYFP-N1 (YFP control) was served as a positive control. Bars = 10 μm.

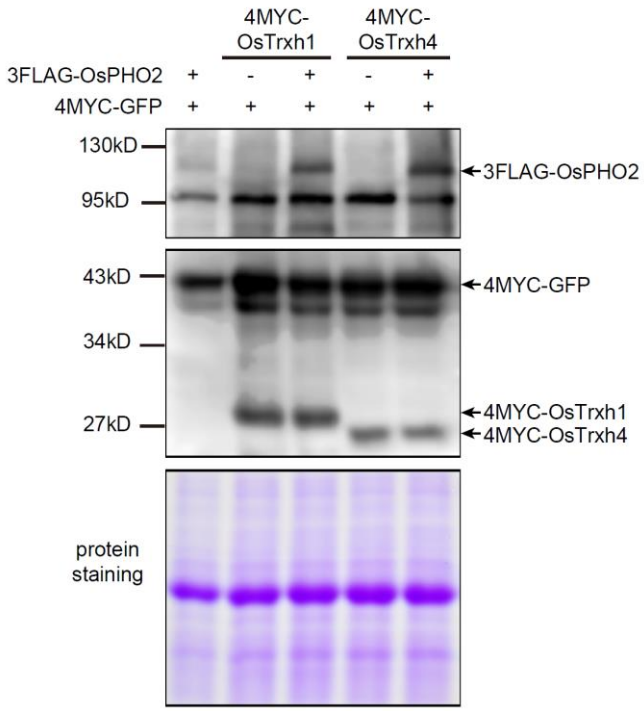

Supplemental Figure S3. OsPHO2 could not target OsTrxh1 and OsTrxh4 to degradation in tobacco leaves.
Co-expression of 3FLAG-tagged OsPHO2 with 4MYC-tagged OsTrxh1 or OsTrxh4. The immunoblots were conducted using the tag specific antibodies. 4MYC-GFP was used as the control for the infiltration event. The bottom panel showed protein staining.

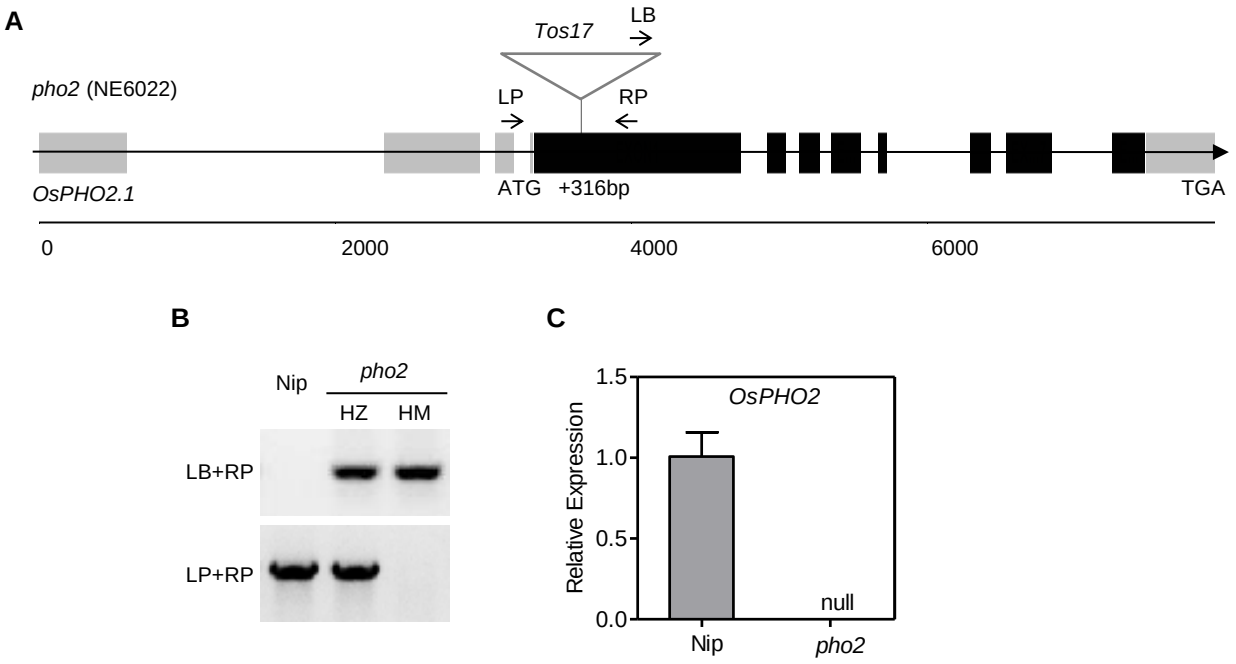

Supplemental Figure S4. Identification of rice *Tos17* insertion mutant *pho2* (NE6022).
A, *OsPHO2* gene structure and the *Tos17* insertion site. The exon region of *OsPHO2.1* is represented with boxes (black, coding region; grey, untranslated region). The *Tos17* insertion site is at +316bp after the ATG code. LB, LP, and RP are primers used in B to identify *pho2* mutant.
B, PCR analysis of the *Tos17* insertion at the first coding exon of *OsPHO2*. HM, homozygous *pho2* mutant; HZ, heterozygous; Nip, wild type *Nipponbare*.
C, qRT-PCR analysis of the *OsPHO2* expression in the wild type (Nip) and *pho2* mutant seedlings.
The primers used for PCR and qRT-PCR analysis are listed in Table S2 and S3.

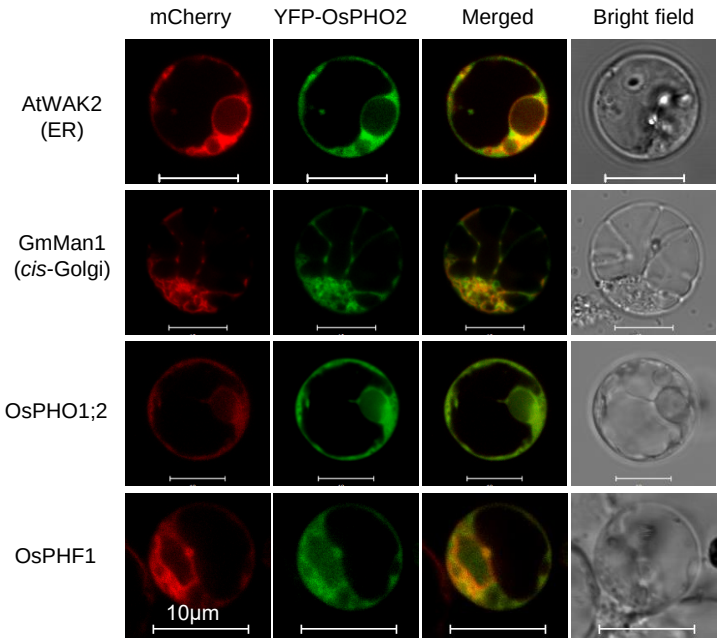

Supplemental Figure S5. Co-subcellular localization of YFP-OsPHO2 with ER/Golgi markers and OsPHF1/OsPHO1;2-mCherry fusion proteins in rice protoplasts.
The ER/Golgi markers were AtWAK2/GmMan1-mCherry, respectively. Bars = 10 μm.

APP	pBT3-STE OsPHO1;2 -Cub	pBT3-STE OsPHF1-Cub	pBT3-N Cub-OsPHO1;2	pBT3-N Cub-OsPHF1	pBT3-STE OsPHO2-Cub	pBT3-N Cub-OsPHO2
pBT3-STE OsPT2-Cub	pBT3-STE OsPT6-Cub	pBT3-STE OsPT8-Cub	pBT3-N Cub-OsPT2	pBT3-N Cub-OsPT6	pBT3-N Cub-OsPT8	

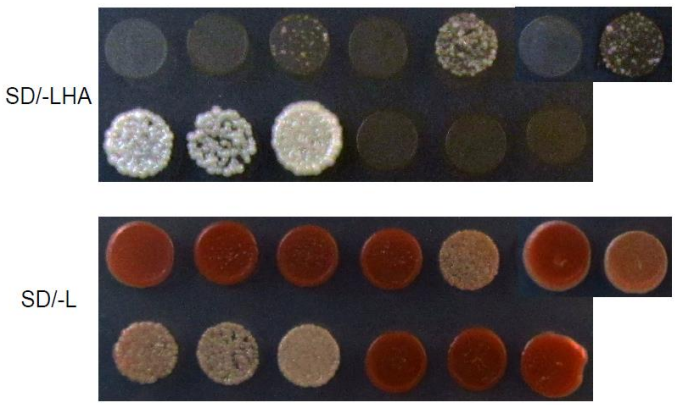

Supplemental Figure S6. Validation of auto activation activities of bait vectors in split-ubiquitin yeast two-hybrid assays. The coding sequences of OsPHO2/OsPHF1/OsPHO1;2 and OsPT2/6/8 were cloned in frame into both pBT3-STE and pBT3-N bait vectors with Cub. The yeast strain NMY51 cells were transformed with these bait constructs and grown on SD/-L (lacking Leu) plates. The auto activation activities of reporter genes were assessed by the growth of yeast colonies on SD/-LHA (lacking Leu, His, and Ade) plates for 3 days.

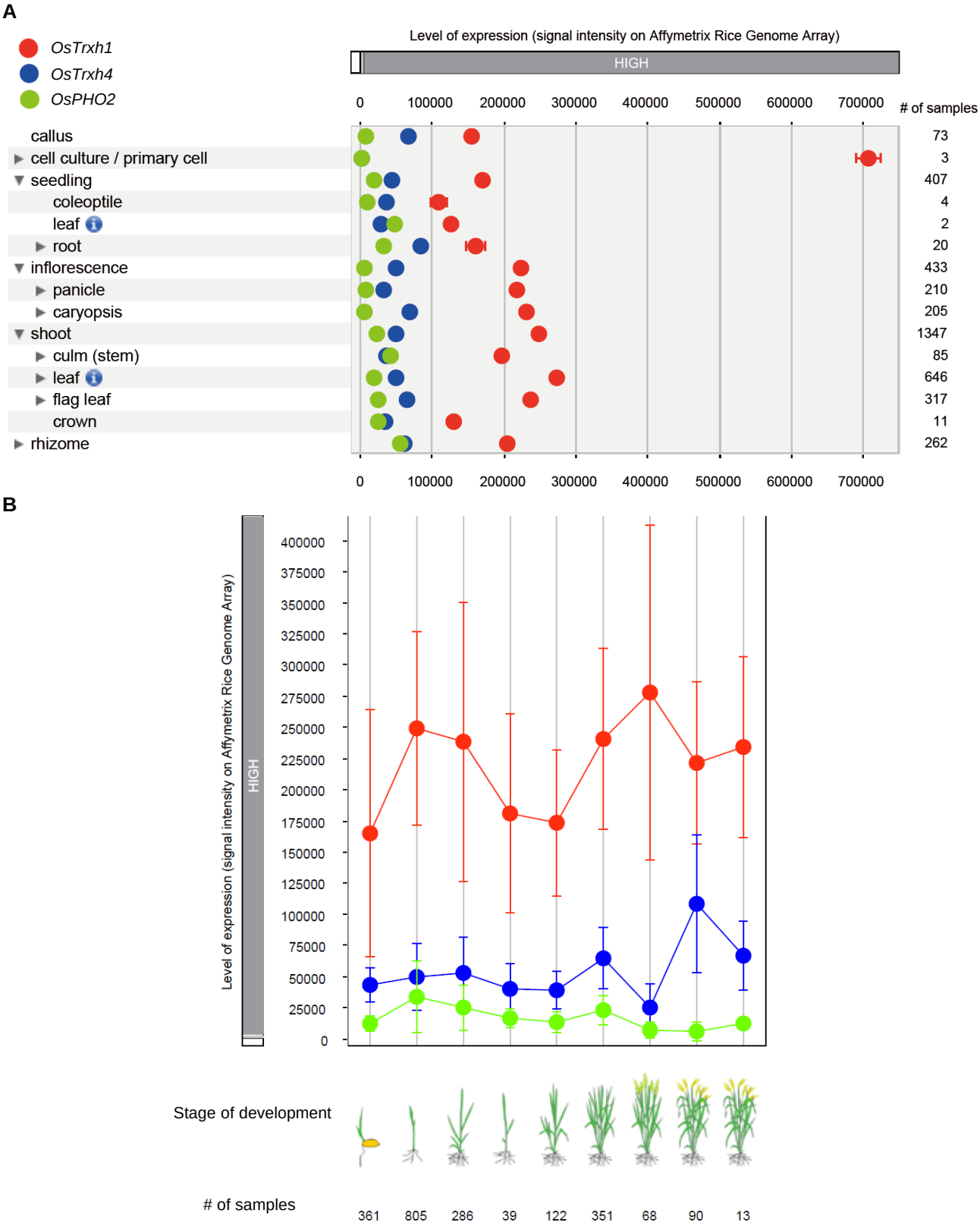

Supplemental Figure S7. Expression levels of *OsTrxh1*, *OsTrxh4* and *OsPHO2* in **(A)** different tissues and **(B)** different development stages based on microarray data retrieved from GENEVESTIGATOR (https://genevestigator.com/gv/).

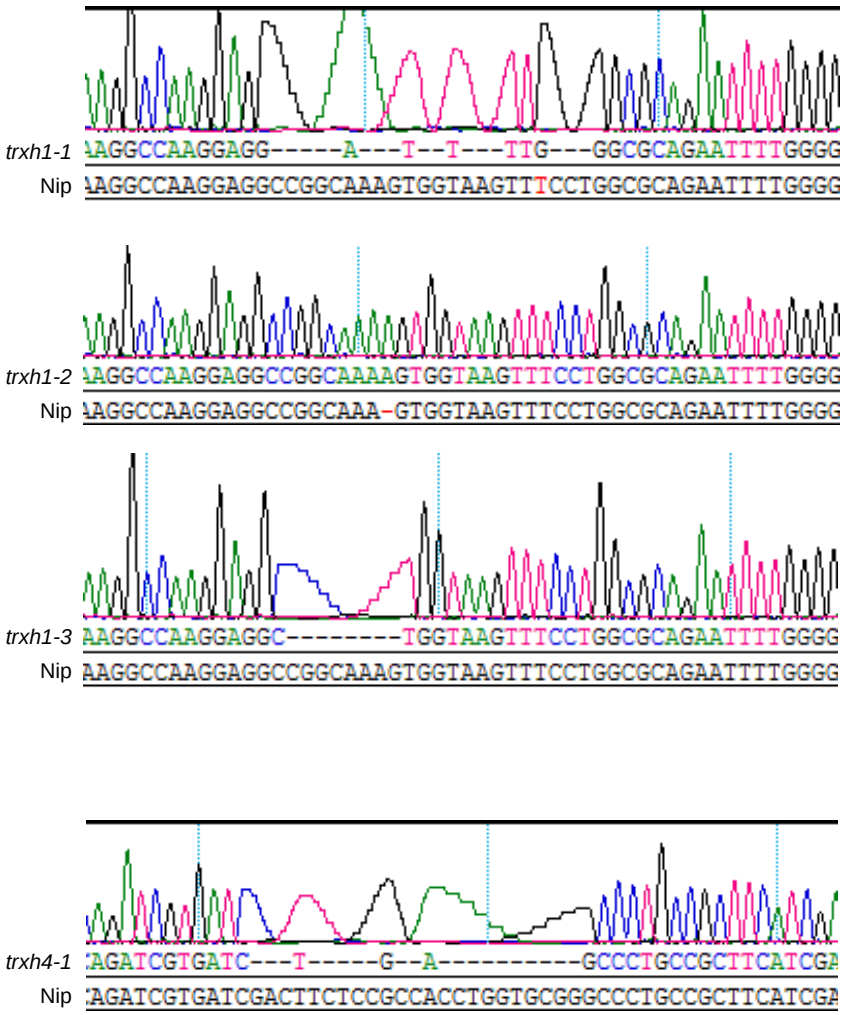

Supplemental Figure S8. Sequencing results of the CRISPR/Cas9 mutants of *OsTrxh1* and *OsTrxh4*.
PCR products were amplified using genomic DNA as template. The primers used to amplify the fragments for sequencing are listed in Table S2.

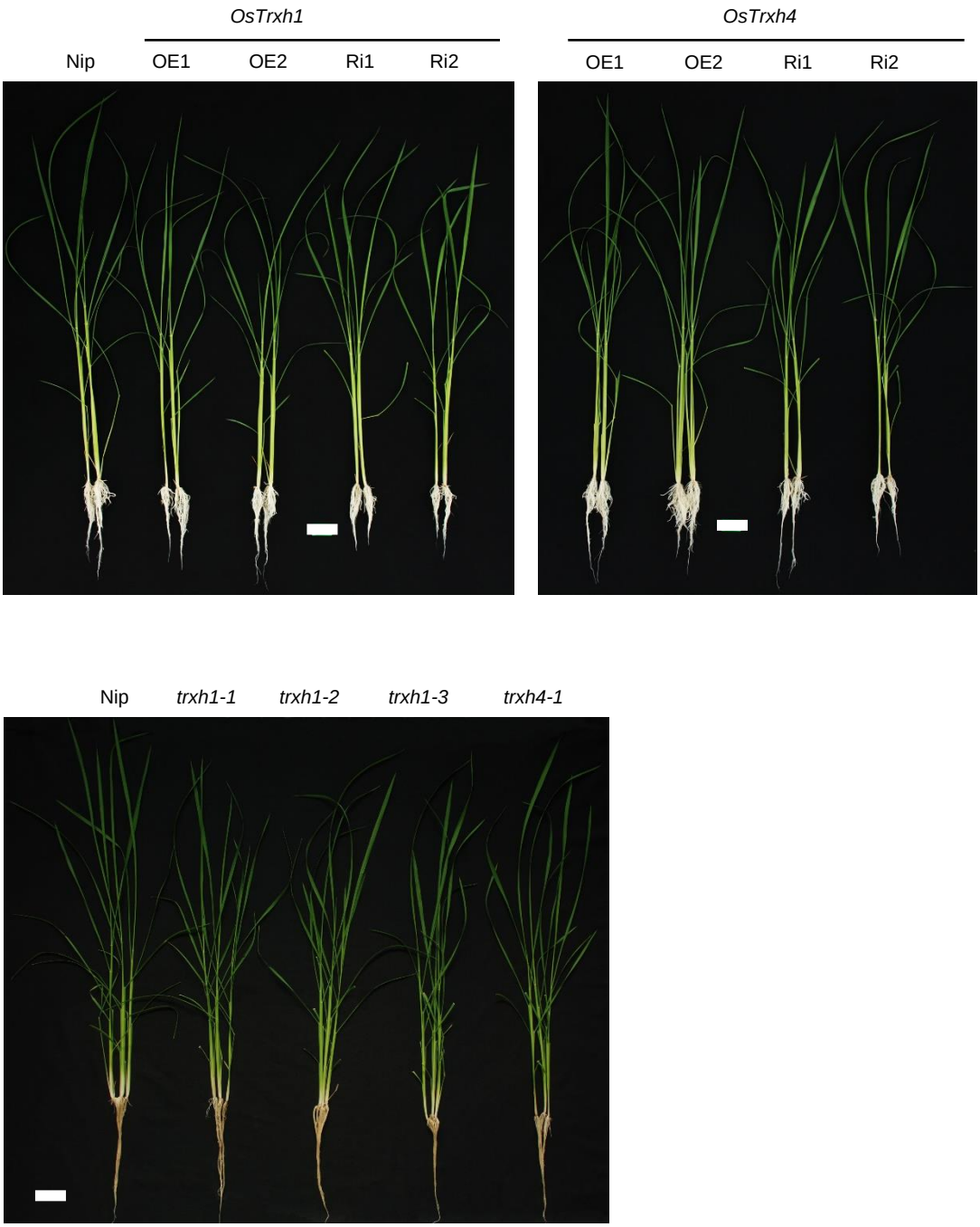

Supplemental Figure S9. Morphological appearance of Nipponbare (Nip), overexpression (OE), RNA interference (Ri) and CRISPR/Cas9 mutants of *OsTrxh1* and *OsTrxh4*.
Rice seedlings were grown in a Pi-sufficient solution (0.32 mM Pi) for 28 days. Bars = 4 cm.

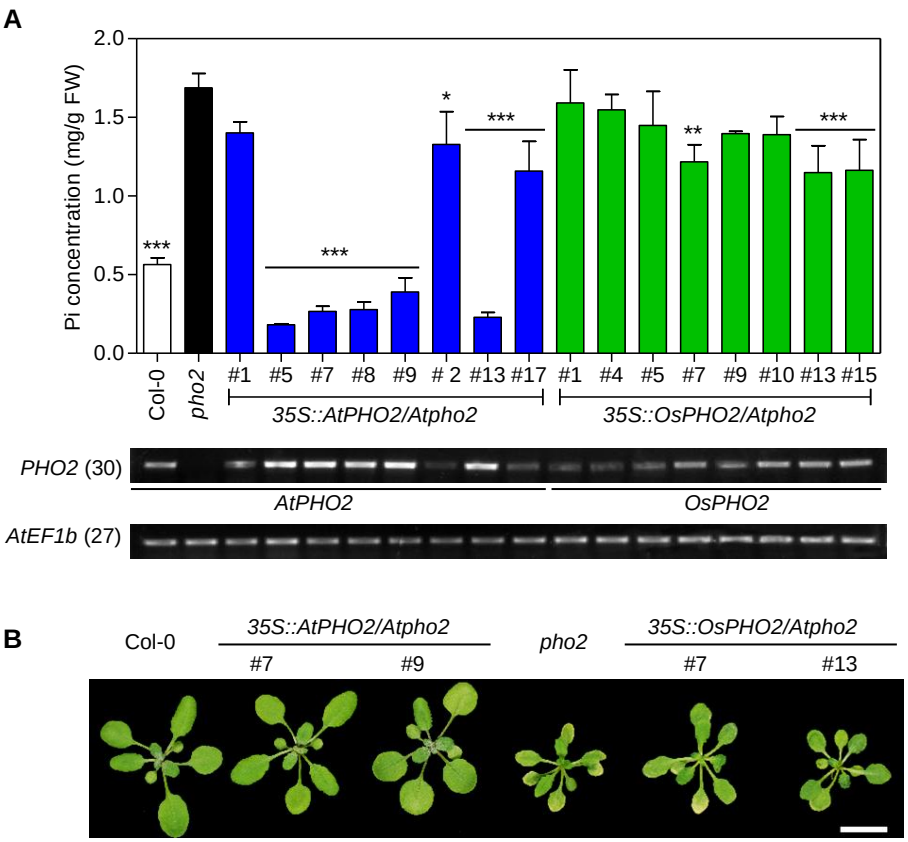

Supplemental Figure S10. Over-expression of *AtPHO2* could restore Arabidopsis *pho2* mutant, whereas over-expression of *OsPHO2* could not.

Transgenic Arabidopsis seedlings were germinated on MS medium with 18 mg/L Hygromycin B and grown for 9 days, then transferred into MS medium for further 9-day-growth before sampled.

A, The Pi concentration in shoots of *AtPHO2* or *OsPHO2* over-expressing transgenic lines in Arabidopsis *pho2* background. Errors bars indicate SD and n = 3. The transcript level of *PHO2* in the wild type (Col-0), *pho2* mutant and transgenic lines over-expressing *AtPHO2* or *OsPHO2* were analyzed by RT-PCR. Expression of *AtEF1b* served as the internal control. Data significantly different from the *pho2* were indicated by asterisks (Dunnett's ANOVA test; *P<0.05, **P<0.01, ***P<0.001).

B, Growth performance of 18-day old seedlings. Bar = 4 cm.

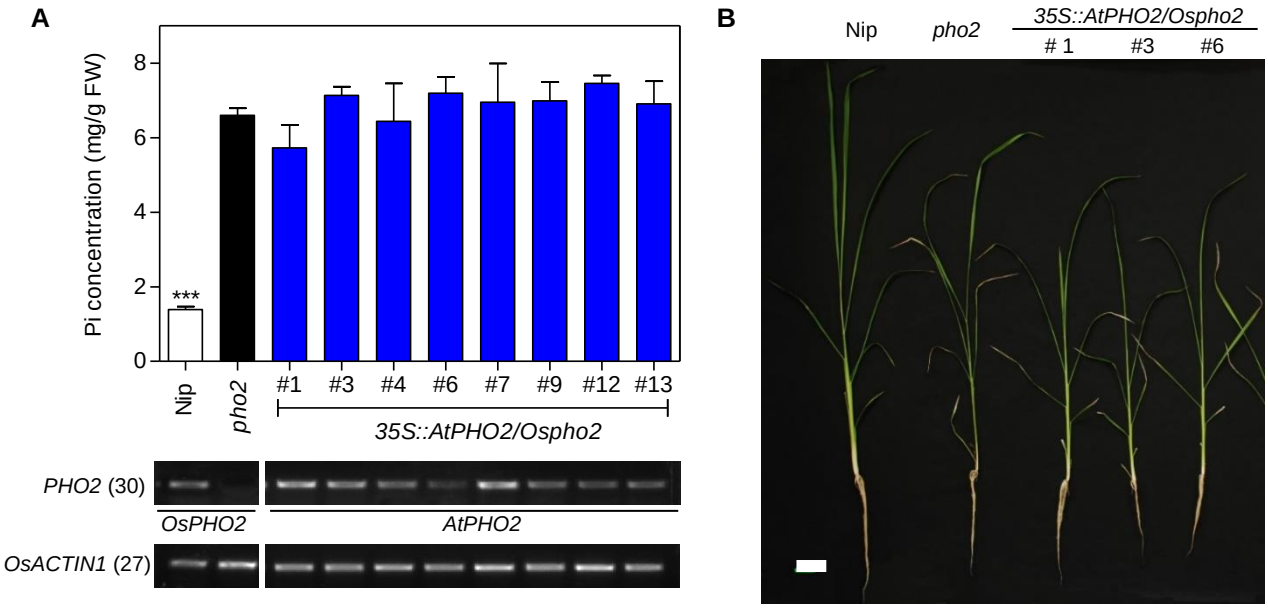

Supplemental Figure S11. Rice *pho2* mutants could not be recovered by expressing 35S::*AtPHO2*.
Rice seedlings were germinated and grown in a Pi-sufficient hydroponic solution (0.32 mM Pi) for 24 days before sampled.
A, The Pi concentration in shoots of *AtPHO2* over-expressing transgenic lines in rice *pho2* background. Errors bars indicate SD and n = 3. The transcript level of *PHO2* in the wild type Nip (*Nipponbare*), *pho2* and *AtPHO2*-over-expressing transgenic lines were analyzed by RT-PCR. Expression of *OsACTIN1* served as the internal control. Data significantly different from the *pho2* were indicated by asterisks (Dunnett's ANOVA test; ***P<0.001).
B, Growth performance of 24-day-old seedlings. Bar = 4 cm.

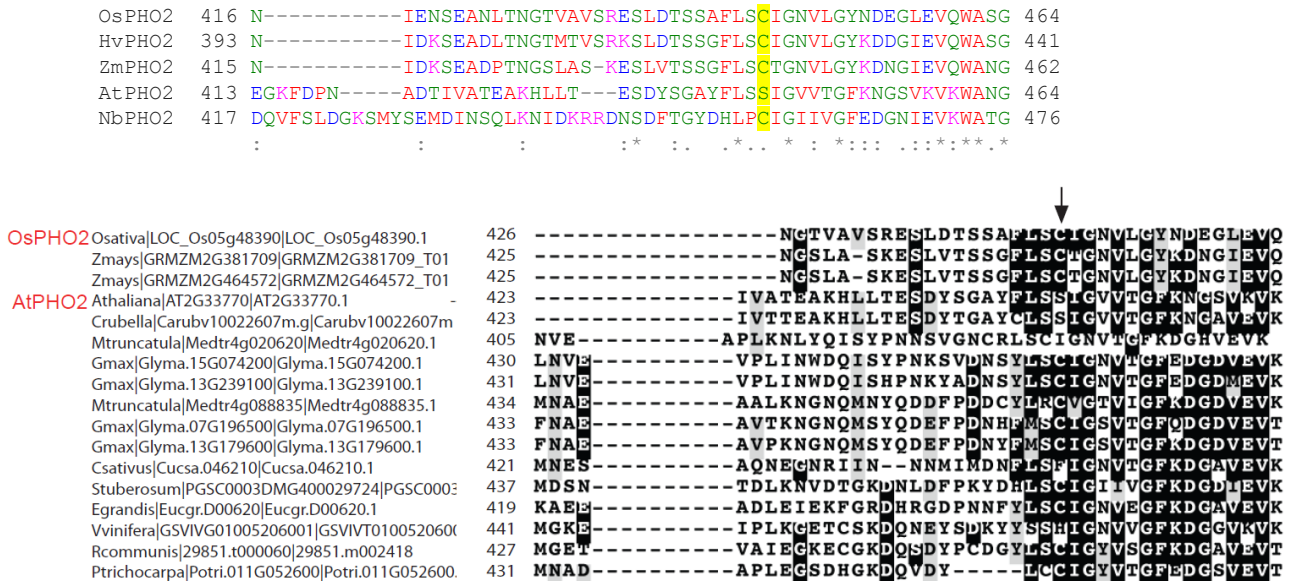

Supplemental Figure S12. Amino acids alignment of PHO2 and PHO2-like proteins in multiple plant species.